

## Quantum motor: Directed wave-packet motion in an optical lattice

Quentin Thommen, Jean Claude Garreau, and Véronique Zehnlé

*Laboratoire de Physique des Lasers, Atomes et Molécules, Université Lille 1 Sciences et Technologies,*

*CNRS, F-59655 Villeneuve d'Ascq Cedex, France\**

(Received 16 April 2011; published 4 October 2011)

We propose a method for arbitrary manipulations of a quantum wave packet in an optical lattice by a suitable modulation of the lattice amplitude. A theoretical model allows us to determine the modulation needed to generate an arbitrary atomic trajectory; wave-packet rotations can also be implemented. The method is immediately usable in state-of-the-art experiments.

DOI: [10.1103/PhysRevA.84.043403](https://doi.org/10.1103/PhysRevA.84.043403)

PACS number(s): 37.10.Jk, 03.65.Aa

### I. INTRODUCTION

The fine manipulation of wave packets is a fundamental requirement in a large number of fields. Important examples are quantum transport [1–5], “quantum simulators” that aim to reproduce solid-state models [6–12], quantum information [13–16], and quantum metrology [17]. The possibility of trapping very cold atoms by light was a decisive step leading to enormous progress in this field. Tailored optical potentials, created by multiple interfering beams, allow us to trap and guide atomic wave packets for long times (compared to the dynamics of the atom external degrees of freedom) and distances (compared to the de Broglie wavelength), and the use of far off-resonance beams reduces decoherence effects to negligible levels. With such techniques, old problems of quantum dynamics have been experimentally studied, such as the elusive Bloch oscillations [18,19] or quantum chaos [20–26]. In the emerging, and rapidly developing, field of quantum information, controlled motion in optical lattices provides ways to manipulate *qubits*, for example, in generating multiparticle entanglement by finely tuned interactions between atoms [27–29]. A relevant point for the development of such techniques is the shaping and displacing of wave packets at will, which is the problem addressed in the present work, where we consider the motion of a wave packet in a driven (modulated) two-dimensional (2D) optical lattice (the generalization to the 3D case is straightforward). By carefully engineering the temporal driving of the optical potential, we demonstrate a way to coherently impinge to an atom in a lattice almost any kind of motion, including rotations of its wave packet. Tailoring of wave-packet dynamics has been previously studied both theoretically [30–32] and experimentally [2,12]. In the present work we show that a *suitable modulation of the driving itself* allows us to displace a wave packet along paths of arbitrary shape with controlled dispersion in any dimension.

### II. DYNAMICS IN TILTED LATTICES: WANNIER-STARK BASIS

Let us first consider the quantum dynamics of an atom in a 1D tilted (or “washboard”) potential formed by a sinusoidal potential superposed on a constant force  $F_x$ . We

use normalized variables in which lengths are measured in units of the lattice step  $d$  ( $=\lambda_L/2$ , with  $\lambda_L = 2\pi/k_L$  being the laser wavelength), energy is in units of the recoil energy  $E_R = \hbar^2 k_L^2 / (2M)$ , where  $M$  is the atom mass, and time is measured in units of  $\hbar/E_R$ . The corresponding Hamiltonian is

$$H_x = -\frac{1}{2m^*} \frac{\partial^2}{\partial x^2} + [V_x + A_x(t)] \cos(2\pi x) + F_x x, \quad (1)$$

where  $m^* = \pi^2/2$  is the mass in normalized units,  $F_x$  is the constant force measured in units of  $E_R/d$ ,  $\hbar = 1$ , and  $V_x$  is the lattice amplitude, to which a time-dependent component  $A_x(t)$  can be added. Tilted optical lattices have been experimentally realized by many groups [2,18,19,33,34].

Dynamics in a tilted lattice is conveniently described by *Wannier-Stark* (WS) states [19,35–38], which are the eigenstates of the Hamiltonian equation (1) with  $A_x(t) = 0$ . In numerical simulations a finite lattice is used, but if the bounds of the lattice are far enough from the region of interest, there is no essential difference in the dynamics. The eigenenergies of the Hamiltonian equation (1) form a “ladder” structure with steps separated by the “Bloch frequency”  $\omega_B \equiv 2\pi/T_B = F_x$  ( $\omega_B = F_x d/\hbar$  is in the usual units), with each step in the ladder corresponding to an eigenfunction centered in a well of the lattice. Depending on  $V_x$  and  $F_x$ , each well can host more than one WS state, and each family of states then forms its own ladder [36]. Throughout this paper the parameters of the potential and the initial conditions are so chosen that the atomic dynamics is accurately described by the *lowest-ladder* WS (ground) states alone. This situation can be realized experimentally by using cold enough atoms and raising the optical potential adiabatically [19]. As WS states are, for the parameters used in the present work, highly localized on the corresponding potential well, we label a WS state by index  $n$  of the well in which it is centered:  $\varphi_n(x)$ . These states are invariant under a translation of an integer number  $n$  of lattice steps, provided the associated energy is also shifted by  $n\omega_B$ , that is,

$$\varphi_n(x) = \varphi_0(x - n) \quad (2)$$

$$E_n = E_0 + n\omega_B \quad (3)$$

(we set  $E_0 = 0$  in the following). It is well known that a wave packet submitted to the Hamiltonian equation (1), with  $A_x(t) = 0$ , has an oscillatory behavior, called the Bloch oscillation, of frequency  $\omega_B$ . Adding a time-dependent potential

\*<http://www.phlam.univ-lille1.fr/atfr/cq>

modulated at (or around) the frequency  $\omega_B$  is thus a good way to create a resonant response in the dynamics. We shall consider here only the resonant dynamics corresponding to a frequency very close to  $\omega_B$ .

We can expand the atomic wave function  $\psi_x(t)$  over the WS (ground) states:

$$\psi_x(t) = \sum_n c_n(t) e^{i\phi_n(t)} \varphi_n(x), \quad (4)$$

where the phase  $\phi_n(t)$  is conveniently defined by

$$\phi_n(t) = -n\omega_B t - V_x M_0 \int_0^t A_x(t') dt', \quad (5)$$

where  $M_0$  is the  $p = 0$  value of the coupling parameter  $M_p$ , defined by

$$M_p \equiv \langle \varphi_i | \cos(2\pi x) | \varphi_{i+p} \rangle = \langle \varphi_0 | \cos(2\pi x) | \varphi_p \rangle. \quad (6)$$

[The last identity is a consequence of Eq. (2).] Bringing Eq. (4) into the Schrödinger equation associated with the Hamiltonian equation (1), one obtains a set of equations:

$$\dot{c}_n(t) = -i A_x(t) \sum_{p \neq 0} M_p c_{p+n} e^{-ip\omega_B t}. \quad (7)$$

We now set in Eq. (1) the driving to

$$A_x(t) = \alpha_x(t) \sin(\omega_B t + \beta_x), \quad (8)$$

where  $\alpha_x(t)$  is assumed to be a *slowly* varying function ( $|\alpha_x^{-1} d\alpha_x/dt| \ll \omega_B$ ). Equations (7) can be simplified by using the following assumptions: (i) as all the frequencies present in the driving  $A_x(t)$  are close to the resonance value  $\omega_B$ , fast oscillations can be neglected, and (ii) for deep enough potential wells,  $M_p \ll M_1$  for  $|p| > 1$ , so that only nearest-neighbor couplings are considered. In what follows, we chose the parameters in the numerical simulations so that these conditions are always satisfied, which allows us to reduce Eq. (7) to

$$\dot{c}_n(t) = \frac{M_1 \alpha_x(t)}{2} [c_{n-1} e^{-i\beta_x} - c_{n+1} e^{i\beta_x}], \quad (9)$$

whose general solution is

$$c_n(t) = \sum_p c_{n+p}(t=0) e^{ip\beta_x} J_p \left( -M_1 \int_0^t \alpha_x(t') dt' \right), \quad (10)$$

where  $J_p(x)$  is the Bessel function of the first kind and order  $p$  [39]. The mean position of the wave packet, averaged over a Bloch period  $T_B$ , is obtained from Eq. (10):

$$\langle x \rangle_t = \langle x \rangle_{t=0} + \int_0^t v_x(t') dt',$$

where

$$v_x(t) = M_1 \alpha_x(t) \text{Re}(\sigma e^{-i\beta_x}) \quad (11)$$

is the instantaneous wave-packet drift velocity and  $\sigma \equiv \sum_p c_p^*(0) c_{p+1}(0)$  is the initial coherence of the wave packet. The wave packet also presents a diffusion characterized by an instantaneous diffusion coefficient  $D(t) \propto [M_1 \alpha_x(t) \text{Im}(\sigma e^{-i\beta_x})]$ . Hence, the motion *and* the diffusion can be controlled by changing the temporal driving amplitude  $\alpha_x$  and phase  $\beta_x$ . The diffusion can be suppressed by choosing  $\beta_x$  so that  $\text{Im}(\sigma e^{-i\beta_x}) = 0$ ; one then obtains a pure translation of the wave packet with a velocity given by Eq. (11),  $v_x(t) = \pm M_1 \alpha_x(t) |\sigma|$  [40]. Conversely, setting  $\beta_x$  so that  $\text{Re}(\sigma e^{-i\beta_x}) = 0$  leads to a purely diffusive motion with no displacement of the wave packet's center of mass.

### III. DIRECTED MOTION IN A MODULATED 2D TILTED LATTICE

Consider now a “square” 2D lattice formed by the interference of two orthogonal pairs of counterpropagating laser beams. The resulting Hamiltonian is separable [30]:  $H_{xy} = H_x + H_y$ , where  $H_x$  is given by Eq. (1) and  $H_y$  is the obvious generalization for the  $y$  coordinate. The solution can thus be written as  $\Psi_{xy}(t) = \psi_x(t) \psi_y(t)$ , and the 2D dynamics is obtained simply by solving two identical 1D Schrödinger equations for each  $\psi_u(t)$  ( $u = x, y$ ), with the corresponding Hamiltonian  $H_u$ . We can induce a controlled 2D motion of the wave packet by choosing suitable lattice modulations  $A_u(t) = \alpha_u(t) \sin(\omega_B t + \beta_u)$ , which in turn generate independently

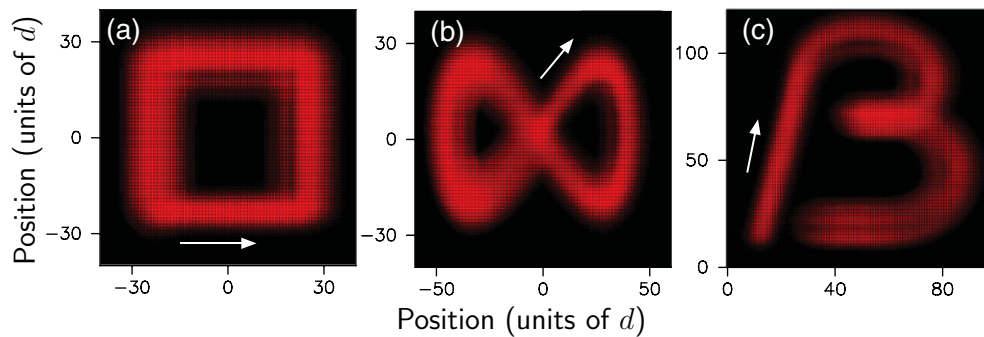


FIG. 1. (Color online) Directed wave-packet motion in two dimensions, obtained by direct integration of the Schrödinger equation. The plots display the probability of presence  $|\Psi_{xy}(t)|^2$  integrated in time, and the arrows indicate the sense of the motion. (a) Square path formed by four straight lines; the motion starts from the left lower corner. (b)  $\infty$  path, obtained by choosing  $\alpha_x = \cos(\Omega t)$ ,  $\alpha_y = \cos(2\Omega t)$ ; the motion starts from the intersection point. (c) The Greek letter  $\beta$  is formed by a combination of straight lines and arcs (motion starts from the tail of the  $\beta$ ). Parameters of the potential are  $V_{x,y} = 2.5$ ,  $F_{x,y} = 0.2$ , and  $\beta_x = \beta_y = 0$  (note the different scales in each plot). The initial wave packet is a Gaussian defined by Eq. (12).

adjustable velocities  $v_x(t)$  and  $v_y(t)$ . Note that we allow  $\alpha_u(t)$  to depend on  $t$ ; that is, we allow the driving amplitude itself to be modulated. In what follows we will consider only the case in which this modulation *of the driving* is slowly varying with respect to frequency of the driving  $\omega_B$ . In order to avoid confusion, we shall call the amplitude modulation at frequency  $\omega_B$  “the driving” and the function  $\alpha_u(t)$  “the modulation of the driving.”

In order to illustrate the possibilities opened by our method, we present in Fig. 1 different trajectories obtained by numerical integration of the Schrödinger equation with an initial wave packet of Gaussian shape:

$$\Psi_{xy}(0) = \sum_{l,m} \exp\left(-\frac{l^2 + m^2}{9}\right) \varphi_l(x) \varphi_m(y). \quad (12)$$

Note that this form implies that  $\sigma$  is real, so that the above “zero-diffusion” condition is fulfilled for  $\beta_x = \beta_y = 0$ . Figures 1(a)–1(c) show the square modulus of the wave packet *integrated in time*, and the arrows indicate the sense of the motion. Figure 1(a) shows a square trajectory obtained with  $\alpha_x = 1$ ,  $\alpha_y = 0$  (and therefore  $v_x = M_1\sigma$ ,  $v_y = 0$ ) for  $0 \leq t \leq 15T_B$ ,  $\alpha_x = 0$ ,  $\alpha_y = 1$  (and therefore  $v_y = M_1\sigma$ ,  $v_x = 0$ ) for  $15T_B \leq t \leq 30T_B$ , and so on. In Fig. 1(b), we drive the

wave packet into an  $\infty$ -shaped Lissajous curve by setting  $\alpha_x(t) = \cos(\Omega t)$ ,  $\beta_x = 0$  and  $\alpha_y(t) = \cos(2\Omega t)$ ,  $\beta_y = 0$ , thus with modulations at frequencies  $\Omega$  and  $2\Omega$  ( $\Omega = \omega_B/250$ ). By combining different types of paths, one can generate any type of trajectories in 2D (a trivial generalization of the above discussion can be obtained in 3D): Fig. 1(c) displays a  $\beta$ -shaped trajectory, where a “turning point” has been “drawn.” In all these numerical experiments, the residual diffusion (see Ref. [40]), which is seen as a progressive thickening of the trajectory, is very small.

New kinds of dynamics can be obtained by modulating the driving with an amplitude that varies slowly also *in space*, i.e.,  $A_x(t) \rightarrow A_x(x,t)$  in Eq. (1). This can be realized [8,41] by adding a second laser beam with a different spatial period  $k'_L$ , which produces a spatial modulation of the lattice amplitude corresponding to the beat note of the two spatial frequencies. The potential is then

$$A_u(u,t) = \sin(ku)(\sin \omega_B t + \beta_u), \quad (13)$$

where  $k = (k_L - k'_L)/k_L$ . In the limit  $|k| \ll 1$ ,  $\sin(ku) \approx ku$  and the velocity of the wave packet, which is proportional to the modulation amplitude, varies linearly with the *position*:  $v_u = M_1\sigma ku$  (taking  $\beta_u = 0$ ), as one can deduce from Eq. (11).

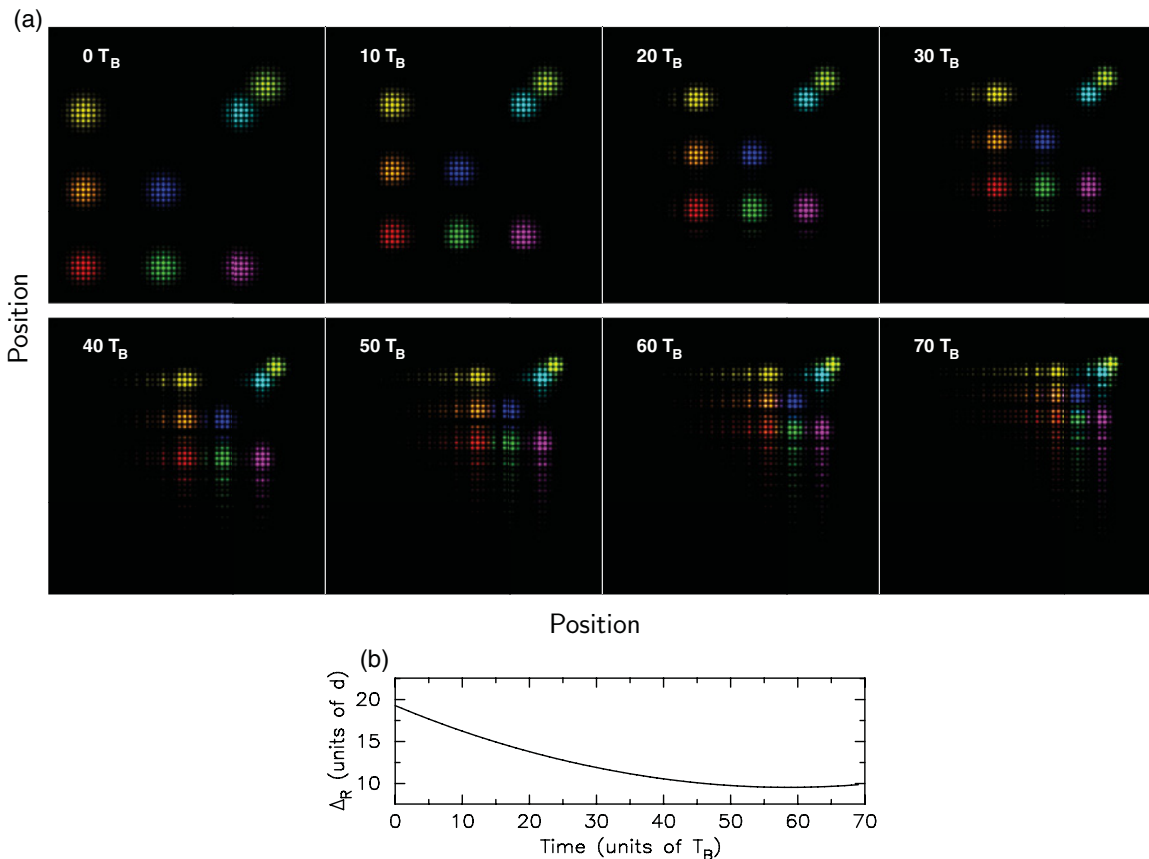


FIG. 2. (Color online) (a) The left plot in the top row displays eight independent atomic wave packets arbitrarily distributed in space. The potential defined by Eq. (13) sets the different wave packets in motion with a velocity directed *toward* the origin (situated close to the top right corner), whose amplitude increases with the distance from the origin. The atoms are thus progressively concentrated around the origin. (b) The evolution of the total spatial dispersion with respect to the origin. Parameters of the potential are  $V_{x,y} = 2.5$ ,  $F_{x,y} = 0.25$ ,  $k/k_L = 0.02$ , and  $\beta_x = \beta_y = 0$ .

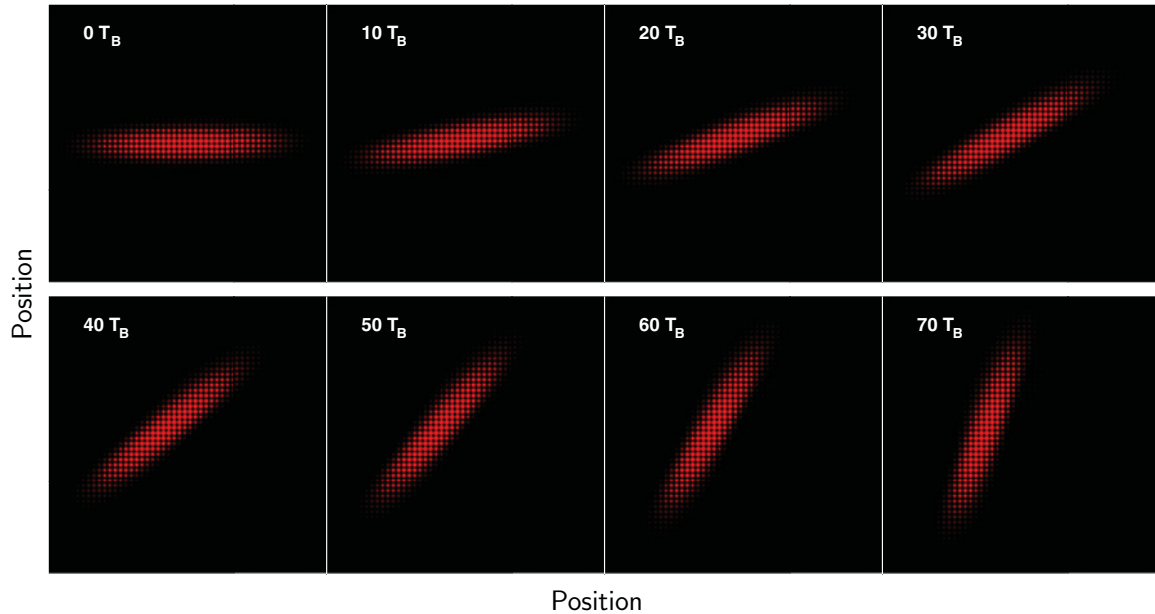


FIG. 3. (Color online) Rotation of the wave packet, obtained by using both a spatial and a temporal modulation of the driving.

A wave packet, whatever its initial position, will move toward the origin  $(0,0)$ , and the closer to the origin it is, the smallest its velocity is. This effect can thus be used to concentrate atomic wave packets centered at arbitrary positions on a few potential wells. Figure 2(a) shows a numerical experiment in which such a concentration is realized. The time evolutions of eight independent wave packets, initially at random positions, are computed independently and are superposed using a different color for each different wave packet. As expected, all wave packets are driven toward the equilibrium position  $(0,0)$  where the amplitude of the modulation of the driving locally vanishes. Figure 2(b) shows the evolution of the total spatial dispersion  $(\langle \Delta r^2 \rangle^{1/2})$ : The fact that the modulation amplitude varies also in space produces a slow diffusion of the wave packets that cannot be suppressed by correctly adjusting the phases  $\beta_u$ ; this residual dispersion is clearly seen in Fig. 2(b) and limits the maximum concentration that can be obtained.

One can also combine temporal and spatial modulations to produce a *rotation* of a wave packet. Consider a cigar-shaped wave packet as shown in the top left plot of Fig. 3. Inducing a uniform rotation around the origin  $(0,0)$  (the geometric center of the wave packet) requires to impinge to the component of the wave packet at position  $\mathbf{r}$  a velocity  $\mathbf{v}$  of modulus proportional

to  $|\mathbf{r}|$  and of direction orthogonal to  $\mathbf{r}$ . This can be done by producing a modulation of the form

$$A_x = -\sin(ky) \sin(\omega_B t + \beta_x) \approx -ky \sin(\omega_B t + \beta_x),$$

$$A_y = \sin(kx) \sin(\omega_B t + \beta_y) \approx kx \sin(\omega_B t + \beta_y).$$

Figure 3 shows an example of the wave-packet rotation produced by such a technique.

#### IV. CONCLUSION

In conclusion, the present work illustrates the possibilities for manipulating extended atomic wave packets, in the weak dispersion regime, by driven optical lattices. The technique is immediately applicable to state-of-the-art experiments. Although we have discussed only 2D examples, which are easier to understand and to display pictorially, generalization of the above discussion to the 3D case is straightforward.

#### ACKNOWLEDGMENTS

Laboratoire de Physique des Lasers, Atomes et Molécules is UMR 8523 of CNRS. Thi work was partially financed by the Agence Nationale de la Recherche (MICPAF project).

- [1] L. Fallani, L. De Sarlo, J. E. Lye, M. Modugno, R. Saers, C. Fort, and M. Inguscio, *Phys. Rev. Lett.* **93**, 140406 (2004).  
 [2] A. Alberti, V. V. Ivanov, G. M. Tino, and G. Ferrari, *Nat. Phys.* **5**, 547 (2009).  
 [3] T. Salger, S. Kling, T. Hecking, C. Geckeler, L. Morales-Molina, and M. Weitz, *Science* **326**, 1241 (2009).  
 [4] F. K. Abdullaev and R. A. Kraenkel, *Phys. Rev. A* **62**, 023613 (2000).

- [5] J. M. Zhang and W. M. Liu, *Phys. Rev. A* **82**, 025602 (2010).  
 [6] M. Greiner, O. Mandel, T. Esslinger, T. W. Hänsch, and I. Bloch, *Nature (London)* **415**, 39 (2002).  
 [7] J. Billy, V. Josse, Z. Zuo, A. Bernard, B. Hambrecht, P. Lugan, D. Clément, L. Sanchez-Palencia, P. Bouyer, and A. Aspect, *Nature (London)* **453**, 891 (2008).  
 [8] G. Roati, C. d'Errico, L. Fallani, M. Fattori, C. Fort, M. Zaccanti, G. Modugno, M. Modugno, and M. Inguscio, *Nature (London)* **453**, 895 (2008).

- [9] B. Deissler, M. Zaccanti, G. Roati, C. d'Errico, M. Fattori, M. Modugno, G. Modugno, and M. Inguscio, *Nat. Phys.* **6**, 354 (2010).
- [10] J. Chabé, G. Lemarié, B. Grémaud, D. Delande, P. Szriftgiser, and J. C. Garreau, *Phys. Rev. Lett.* **101**, 255702 (2008).
- [11] G. Lemarié, H. Lignier, D. Delande, P. Szriftgiser, and J. C. Garreau, *Phys. Rev. Lett.* **105**, 090601 (2010).
- [12] E. Haller, R. Hart, M. J. Mark, J. G. Danzl, L. Reichsöllner, and H. C. Nägerl, *Phys. Rev. Lett.* **104**, 200403 (2010).
- [13] C. Monroe, D. M. Meekhof, B. E. King, and D. J. Wineland, *Science* **272**, 1131 (1996).
- [14] C. Monroe, *Nature (London)* **416**, 238 (2002).
- [15] K. F. Lee, D. M. Villeneuve, P. B. Corkum, and E. A. Shapiro, *Phys. Rev. Lett.* **93**, 233601 (2004).
- [16] A. Lengwenus, J. Kruse, M. Schlosser, S. Tichelmann, and G. Birkl, *Phys. Rev. Lett.* **105**, 170502 (2010).
- [17] J. Ye, H. J. Kimble, and H. Katori, *Science* **320**, 1734 (2008).
- [18] M. Ben Dahan, E. Peik, J. Reichel, Y. Castin, and C. Salomon, *Phys. Rev. Lett.* **76**, 4508 (1996).
- [19] S. R. Wilkinson, C. F. Bharucha, K. W. Madison, Q. Niu, and M. G. Raizen, *Phys. Rev. Lett.* **76**, 4512 (1996).
- [20] F. L. Moore, J. C. Robinson, C. F. Bharucha, B. Sundaram, and M. G. Raizen, *Phys. Rev. Lett.* **75**, 4598 (1995).
- [21] H. Lignier, J. Chabé, D. Delande, J. C. Garreau, and P. Szriftgiser, *Phys. Rev. Lett.* **95**, 234101 (2005).
- [22] J. Ringot, P. Szriftgiser, J. C. Garreau, and D. Delande, *Phys. Rev. Lett.* **85**, 2741 (2000).
- [23] I. Talukdar, R. Shrestha, and G. S. Summy, *Phys. Rev. Lett.* **105**, 054103 (2010).
- [24] P. H. Jones, M. Goonasekera, D. R. Meacher, T. Jonckheere, and T. S. Monteiro, *Phys. Rev. Lett.* **98**, 073002 (2007).
- [25] D. Witthaut, M. Werder, S. Mossmann, and H. J. Korsch, *Phys. Rev. E* **71**, 036625 (2005).
- [26] M. Sadgrove and S. Wimberger, *New J. Phys.* **11**, 083027 (2009).
- [27] D. Jaksch and P. Zoller, *Ann. Phys. (N.Y.)* **315**, 52 (2005).
- [28] P. Marte, R. Dum, R. Taieb, P. Zoller, M. S. Shahriar, and M. Prentiss, *Phys. Rev. A* **49**, 4826 (1994).
- [29] Y. Miroshnychenko, W. Alt, I. Dotsenko, L. Förster, M. Khudaverdyan, D. Meschede, and D. S. Rauschenbeutel, *Nature (London)* **442**, 151 (2006).
- [30] D. Witthaut, F. Keck, H. J. Korsch, and S. Mossmann, *New J. Phys.* **6**, 41 (2004).
- [31] A. Alberti, G. Ferrari, V. V. Ivanov, M. L. Chiofalo, and G. M. Tino, *New J. Phys.* **12**, 065037 (2010).
- [32] V. V. Ivanov, A. Alberti, M. Schioppo, G. Ferrari, M. Artoni, M. L. Chiofalo, and G. M. Tino, *Phys. Rev. Lett.* **100**, 043602 (2008).
- [33] B. P. Anderson and M. Kasevich, *Science* **282**, 1686 (1998).
- [34] A. Zenesini, H. Lignier, G. Tayebirad, J. Radogostowicz, D. Ciampini, R. Mannella, S. Wimberger, O. Morsch, and E. Arimondo, *Phys. Rev. Lett.* **103**, 090403 (2009).
- [35] G. H. Wannier, *Phys. Rev.* **117**, 432 (1960).
- [36] Q. Thommen, J. C. Garreau, and V. Zehnlé, *Phys. Rev. A* **65**, 053406 (2002).
- [37] H. L. Haroutyunyan and G. Nienhuis, *Phys. Rev. A* **64**, 033424 (2001).
- [38] M. Glück, M. Hankel, A. R. Kolovsky, and H. J. Korsch, *Phys. Rev. A* **61**, 061402(R) (2000).
- [39] Q. Thommen, J. C. Garreau, and V. Zehnlé, *J. Opt. B: Quantum Semiclass. Opt.* **6**, 301 (2004).
- [40] Note that the above expression for  $D(t)$  is valid in the limit of a spatially smooth wave packet [36]; for wave packets spreading over a few potential wells such as those used in the numerical simulations there is a small residual diffusion, visible on the figures, even if the zero-diffusion condition is satisfied.
- [41] G. G. Carlo, G. Benenti, G. Casati, S. Wimberger, O. Morsch, R. Mannella, and E. Arimondo, *Phys. Rev. A* **74**, 033617 (2006).